Master's Degree Thesis
ISRN: HK/R-IMA-EX--1998/D-03--SE

Crack Detection using Non-linear and Dissipative Acoustics

Daniel Carldén
Daniel Thuresson

Department of Mechanical Engineering
University of Karlskrona/Ronneby
Karlskrona, Sweden
1998

Supervisor: Claes Hedberg, Ph.D. Mech. Eng.

Crack Detection using Non-linear and Dissipative Acoustics

Daniel Carldén
Daniel Thuresson

Department of Mechanical Engineering
University of Karlskrona/Ronneby
Karlskrona, Sweden
1998

Thesis submitted for completion of Master of Science in Mechanical Engineering with emphasis on Structural Mechanics at the Department of Mechanical Engineering, University of Karlskrona/Ronneby, Karlskrona, Sweden.

Abstract:
A theoretical model for identification of acoustical non-linearity using Burger's equation was implemented in a MATLAB program. The program identified both the non-linearity parameter and the distance from the signal source. Tests were performed in order to verify the theories. Tests with a steel bar showed no detectable non-linearity, probably due to insufficient wave amplitude by the signal source. A crack model was made with successful result.

Keywords:
Non-linear acoustics, Non-linear parameter, Burger's equation, Bessel-Fubini, Fay, Mendousse, Hedberg, Non-destructive testing (NDT), Non-destructive Evaluation (NDE), crack detection,

Acknowledgements

This work was carried out at the Department of Mechanical Engineering at the University of Karlskrona/Ronneby, under the supervision of Dr. Claes M. Hedberg.

We wish to express our gratitude to Dr. Claes M. Hedberg for his guidance and advice throughout our work.

We would also like to thank our friends and fellow students for their support during this project.

Karlskrona, October 1998

Daniel Carldén

Daniel Thuresson

Contents

1 Notation

A	Material parameter
a_m	Coefficient
B	Material parameter
b	Dissipation
c_0	Low amplitude signal sound speed
$I_{n,m}$	Integral quantity
i	Imaginary unit
J_n	Bessel function
ksps	Kilo Samples Per Second
Msps	Mega Samples Per Second
m	Integer
n	Integer
p	Pressure
p_0	Equilibrium pressure
t	Time
t_1	Time
t_2	Time
V	Dimensionless velocity
V_0	Dimensionless boundary velocity
v	Velocity
v_0	Source velocity amplitude
x	Propagated distance
β	Non-linear parameter
ε	Non-linearity over dissipation ratio
θ	Dimensionless retarded time
θ_0	Integration variable
θ_d	Integration limit
ρ	Density
ρ_0	Equilibrium density
σ	Dimensionless propagated distance
τ	Retarded time
ω	Angular frequency

2 Introduction

Great interest in non-linear acoustics has been expressed recently in the investigation of micro-inhomogeneous media exhibiting high acoustic non-linearity. The interest of such media is, among other things, due to the possibility of using non-linear effects for non-destructive testing. The conventional methods of non-destructive testing utilise the measurement of linear acoustic parameters of the investigated media; i.e. the excitation and the reception of the wave have the same frequencies. The influence of cracks on the propagation and scattering of linear waves have been discussed in many books and articles, for example [3]. Recently, non-linear vibro-acoustic methods have been investigated in which the excited and received frequencies are different [8,12,13]. These methods provide new opportunities for detecting various defects in materials. The basic concept of the proposed methods is simple: materials containing defects have a much larger non-linear response than materials with no defects. Metals containing very small cracks are easily detected with non-linear analysis. The non-linear parameter for a micro-inhomogeneous material can be 10-1000 times higher than for the same material with no defects.

The aim of this work is to investigate a method for non-linear analysis suggested by our supervisor Claes M. Hedberg, which is described in chapter 3. A program for identification of non-linearity, using Burgers' equation, is made in MATLAB. Empirical testing of a non-linear material is conducted in order to verify the theories.

There are existing methods of non-linear investigations such as those suggested by A. Sutin [12,13]. One of these methods, using two input frequencies, is also briefly investigated. This investigation is purely empirical and no theoretical interpretations are made.

2.1 Non-Linear Acoustics

Sound waves are made up of density fluctuations in a medium. That medium can be for example air, water or metal. Depending on the medium the sound behaves differently. The most obvious difference is the

speed of sound, which varies in a wide range for different mediums. While sound propagates it will change. It is stronger closer to the signal source, mostly because of geometrical spreading into a larger volume but also because of energy loss to the medium. The sound waves are attenuated. High frequencies are over a distance attenuated more than lower ones. For example if you have been close to jet-aeroplane you know that there are some high tones shrieking. When the jet is in the sky however, you hear mostly low frequencies.

Sometimes different frequencies travel with different speed in the same medium. This is called dispersion. Dispersion is neglected in this paper.
If waves with different amplitudes propagate with different speeds we call the wave non-linear.

Most mediums usually have a linear elastic behaviour; i.e. the compression of the media is proportional to the pressure. Acoustic non-linear effects occur when the media no longer have a linear elastic behaviour. Examples of such media are liquids containing gas bubbles, granular, porous, and polycrystalline media.

The main reason for a media such as steel being non-linear is that it contains cracks. Large enough wave amplitude will make the crack open and close, i.e. change the efficient cross-section area, see Figure 2.1. This affect the elasticity since the spring constant is proportional to the efficient cross-section area.

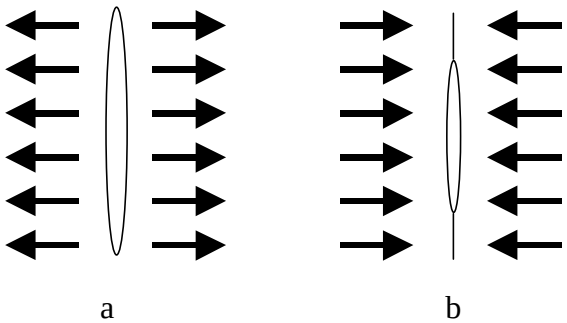

Figure 2.1. a) Crack opening, decreasing contact surface. b) Crack closing, increasing contact surface.

This phenomenon will eventually change the waveform from sinusoidal into a sawtooth profile with increasing distance from the signal source.

This change of shape of the wave can be used to detect non-linearity. When a perfect sawtooth shape is achieved, the wave will give rise to shock waves. An example of a wave propagated through a non-linear media is seen in Figure 2.2.

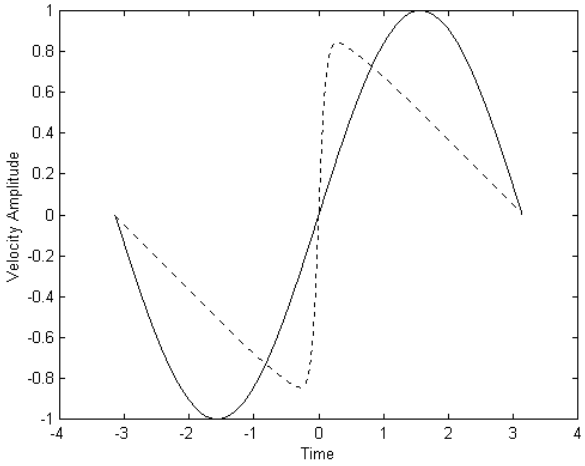

Figure 2.2. Input signal and propagated signal (dashed line).

In Figure 2.3 and Figure 2.4 the frequency spectra (FFT-analysis) of the two signals are shown.

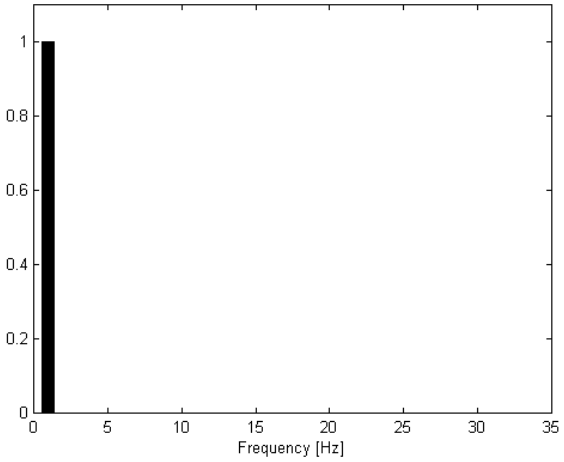

Figure 2.3. FFT-analysis input signal.

In Figure 2.4, the typical high frequency content of a wave propagated through a non-linear media is shown.

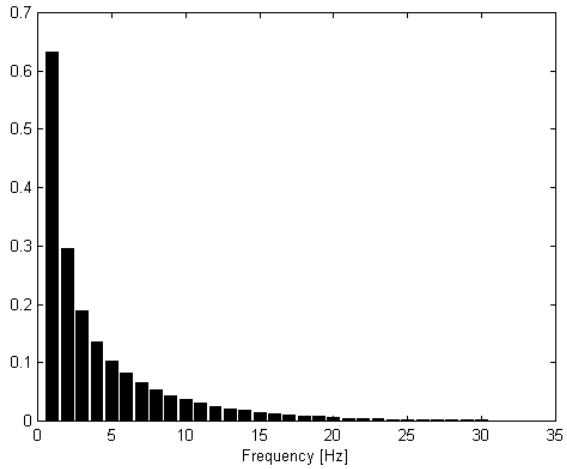

Figure 2.4. FFT-analysis propagated signal.

The process of shock wave formation is counteracted by dissipative factors – viscosity and thermal conductivity – as well as propagation and speed dispersion. These factors lead to a more sinusoidal shape of the wave profile. Correspondingly, the spectral composition undergoes a change: shock wave formation give rise to high frequency harmonic generation, while dissipation results in faster damping of the wave spectrum high-frequency components. Thus, the wave evolution is determined by the competing factors of non-linearity, dissipation and dispersion.

3 Method of Non-linear analysis

The main idea is to assume that every half-period has originated from a signal consisting of a small number of harmonic frequencies. Every half-period is extended so that a full period is obtained. A Fourier analysis (FFT) is performed for each of these periods. To determine the dimensionless dissipation over non-linearity ratio and the dimensionless distance, the Fourier-coefficients are then compared with reference Fourier-coefficients calculated theoretically from Burgers' equation. This is done for several periods and an average is calculated. The reference Fourier-coefficients is calculated using two different solutions to Burgers' equation. These coefficients forms matrices which are used to determine the above mentioned parameters of a measured signal.

4 Theoretical Model

Burgers' equation (4.1) is to be used for this investigation. The reason for this is that Burgers' equation can handle a media with both non-linear and dissipative effects, however, it neglects diffraction. This version of the equation is one-dimensional.

Burgers' equation is often expressed non-dimensionally according to equation 4.1. For a description of the derivation of Burgers' equation, see [10] p. 7-9.

$$\frac{\partial V}{\partial \sigma} - V\frac{\partial V}{\partial \theta} - \varepsilon\frac{\partial^2 V}{\partial \theta^2} = 0 \qquad (4.1)$$

Where the dimensionless quantities are

Velocity:

$$V = \frac{v}{v_0} \qquad (4.2)$$

Propagated distance:

$$\sigma = \frac{\omega v_0 x \beta}{{c_0}^2} \qquad (4.3)$$

Retarded time:

$$\theta = \omega\tau \qquad (4.4)$$

Where

$$\tau = t - \frac{x}{c_0} \qquad (4.5)$$

Non-linearity over dissipation ratio:

$$\varepsilon = \frac{b\omega}{2\beta c_0 v_0 \rho_0} \tag{4.6}$$

Where

$$\beta = 1 + \frac{B}{2A} \tag{4.7}$$

In which A and B are coefficients in the equation of state:

$$p = p_0 + A\frac{\rho - \rho_0}{\rho_0} + \frac{B}{2}\left[\frac{\rho - \rho_0}{\rho_0}\right]^2 + \ldots \tag{4.8}$$

The true quantities are: v is the velocity for the measured point, v_0 is the source velocity amplitude, ω is the angular frequency, x is the propagated distance, β is a non-linearity measure, c_0 is the low amplitude signal sound speed, τ is the retarded time, t is the time, b is a dissipation measure, p_0 is the equilibrium pressure, p is the pressure, ρ_0 is the equilibrium density and ρ is the density.

For a single harmonic continuous boundary condition, $V_0=\sin\theta$, Burgers' equation has several different solutions, which hold for different parts of the solution domain. Four of them are investigated here, namely the Bessel-Fubini, Fay, Mendousse and Hedberg solutions.

The Bessel-Fubini (1935) and Fay (1931) solutions are both analytical but they apply on different distances (σ) from the signal source, Bessel-Fubini (4.9) σ <1 and Fay (4.10) σ >3. Note that the Bessel-Fubini solution neglects dissipation.

$$V_{Bessel-Fubini} = \sum_{n=1}^{\infty} \frac{2J_n(n\sigma)\sin(n\theta)}{n\sigma} \tag{4.9}$$

$$V_{Fay} = \varepsilon \sum_{n=1}^{\infty} \frac{2\sin(n\theta)}{\sinh(n\varepsilon(1+\sigma))} \tag{4.10}$$

Where J_n is a Bessel function.

For the derivation of (4.9) see [5] and (4.10) see [4].

There is a general solution, which in theory is valid for all distances and non-linear over dissipation ratio, namely the Mendousse solution.
This solution (4.11) was presented in 1964. Because of poor convergence of the Bessel function series, the solution is not stable when both ε and σ are small, see [2].

$$V_{Mendousse} = 2i\omega\varepsilon \frac{\sum_{n=-\infty}^{\infty} nJ_n e^{-n^2\omega^2\sigma\varepsilon} e^{in\omega\theta}}{\sum_{n=-\infty}^{\infty} J_n e^{-n^2\omega^2\sigma\varepsilon} e^{in\omega\theta}} \tag{4.11}$$

For the derivation of (4.11) see [9].

The Hedberg solution is an integral method and holds for all σ and neglects dissipation. This solution is numerically equivalent to an earlier solution by Blackstock [1].

$$V_{Hedberg} = \sum_{m=1}^{\infty} a_m \sin(m\theta) \tag{4.12}$$

Where

$$a_m = -\frac{1}{\pi}\left[I_{m-1,m} - I_{m+1,m} + \frac{\sigma}{2} I_{m-2,m} - \frac{\sigma}{2} I_{m+2,m} \right] \tag{4.13}$$

$$I_{n,m} = \int_0^{\theta_d} \cos(n\theta_0 + \sigma m \sin\theta_0) d\theta_0 \tag{4.14}$$

The integration limit θ_d is found by, for the first root larger than zero solving

$$\pi = \theta_d + \sigma \sin\theta_d \tag{4.15}$$

For the derivation of (4.12)-(4.15), see [6] Paper 5, p. 3-6.

Eq. (4.11) and eq. (4.12) is used for this investigation. Eq. (4.12) is used for ε =0 only. The reason for choosing these solutions over Bessel-Fubini and Fay is that they apply for all σ.

4.1 Calculation of Reference Fourier-coefficients

To calculate the reference Fourier-coefficients, eq. (4.11) and (4.12) are used in their respective region of application. The calculation of Fourier-coefficients (1-10) with known ε and σ is done to enable the comparison of a measured signal, and thereby determine a propagated signal's ε and σ. The procedure is described in chapter 4.2. Eq. (4.11) is used for all σ and ε from 0.04 to 1. As this solution becomes unstable with small ε and σ, eq. (4.12) is used for ε =0. The gap between ε=0 and ε =0.04 is interpolated using cubic interpolation so that this gap is filled. Now a complete matrix for each Fourier-coefficient with ε and σ as variables exists. Each coefficient is then divided with the first to obtain the non-dimensional values of the coefficients. This will make the identification of ε and σ easier, since the dependence of signal amplitude is now eliminated. A plot of such a matrix is seen in Figure 4.1.

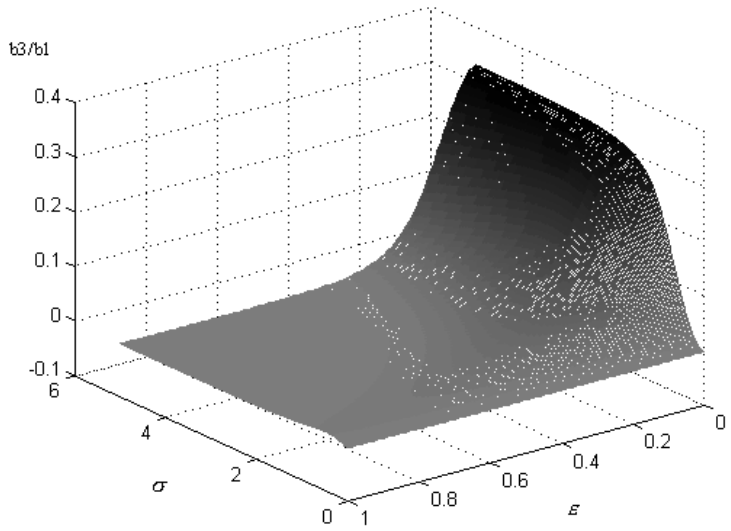

Figure 4.1. Fourier-coefficient ratio for the 3rd Fourier-coefficient, σ and ε as variables.

4.2 The analysis

Every half-period of the measured signal is extended so that a full period is obtained. An FFT-analysis is performed for each of these periods. As in the theoretical calculations, each Fourier-coefficient is divided with the first one. These ratios are compared with their respective calculated equivalence. A measured ratio corresponds to certain level in the calculated $\sigma\varepsilon$-matrix, see Figure 4.2. This forms a curve in the $\sigma\varepsilon$-plane, see Figure 4.3. Such curves are calculated for two different Fourier-coefficient ratios. These curves will at some point cross each other, see Figure 4.4. The crossing-point determines ε and σ. To get as accurate result as possible, several periods of the measured signal is used and then an average is calculated for ε and σ.

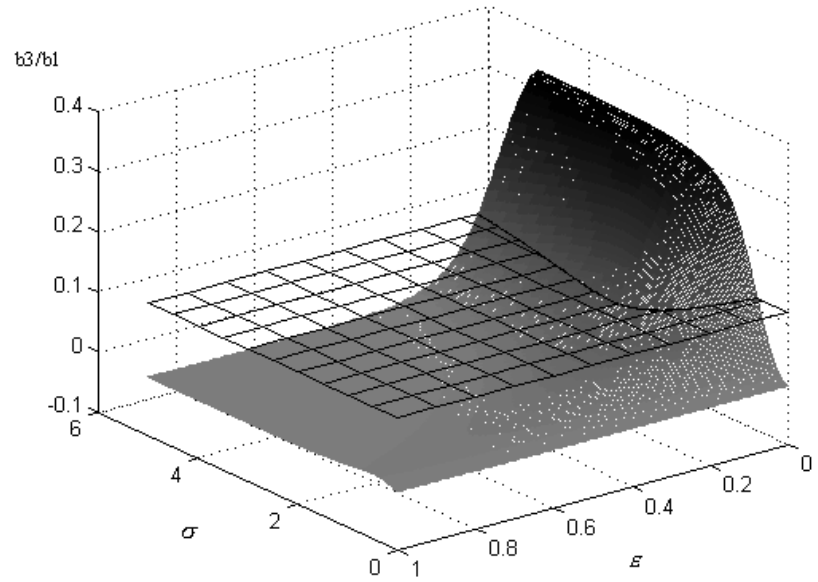

Figure 4.2. Fourier-coefficient level.

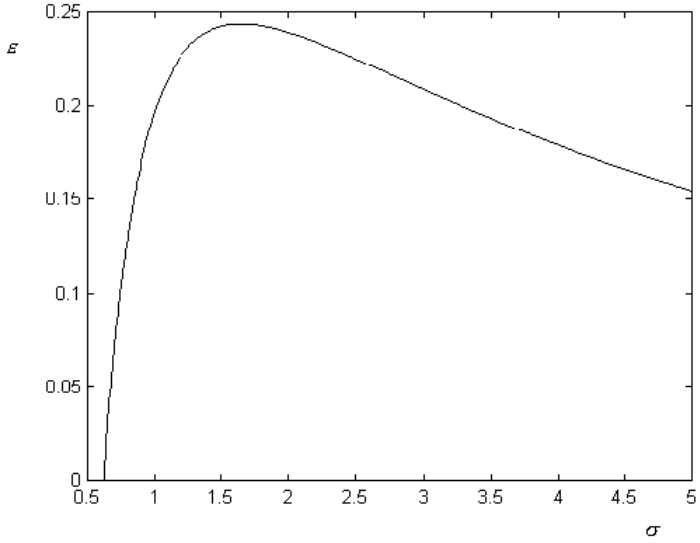

Figure 4.3. ISO-level curve in the σε-plane.

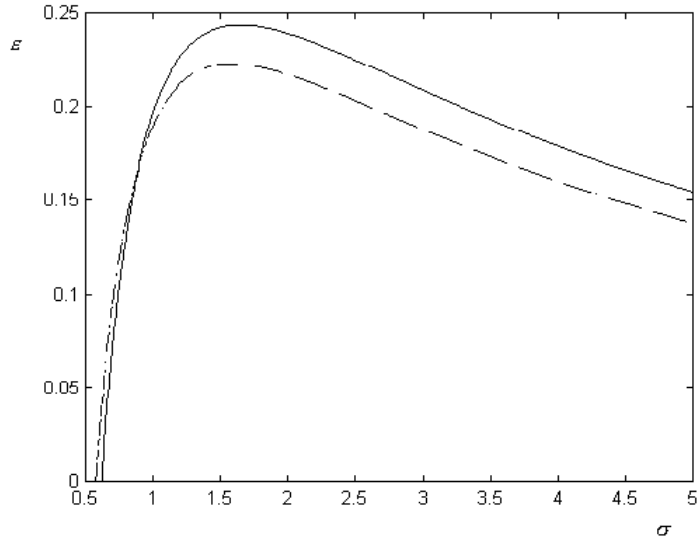

Figure 4.4. ISO-level curves, b3/b1 and b5/b1.

5 Application of Theoretical Model in MATLAB

The main-program made in MATLAB contains five steps.

The first step imports a measured signal into the program and conditions the signal. Offset etc. is compensated for. The signal is also integrated since the measured signal property is acceleration; Burgers' equation uses the velocity.

The second step calculates the Nyqvist frequency, which equals half the sampling frequency.

The third step finds the positions where the signal crosses the zero-value by linear interpolation, see Figure 5.1. This operation is performed in order to find the positions where the signal is to be divided, according to theories in chapter 3.

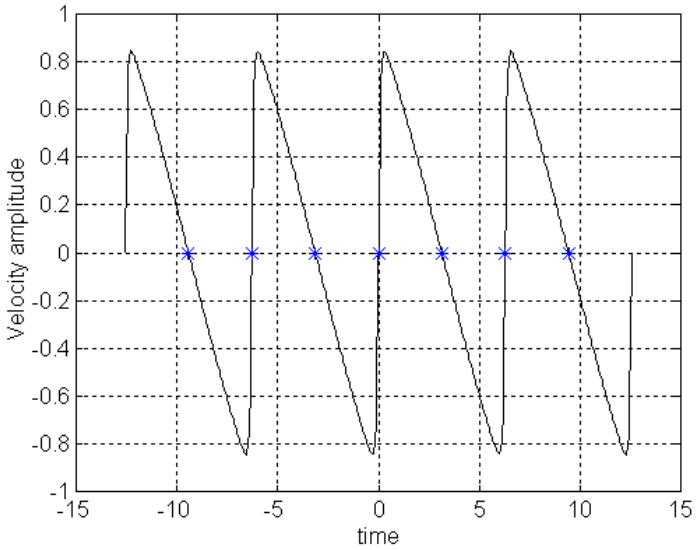

Figure 5.1. Zero positions for measured signal.

Step four divides the signal in half periods, which are extended so that full periods are obtained, see Figure 5.2. An FFT-analysis is performed on each period to obtain the Fourier-coefficients.

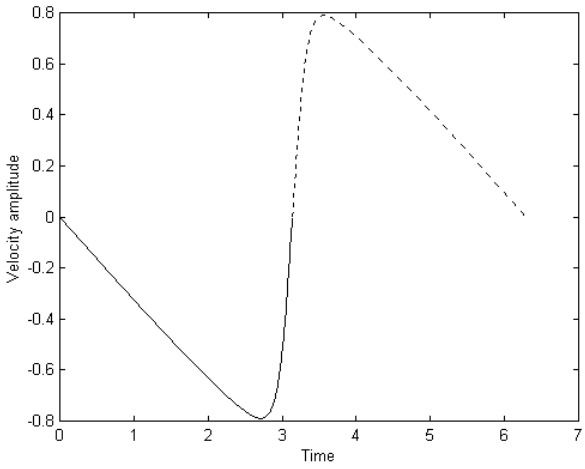

Figure 5.2. Half period (solid line) extended to retrieve a full period.

The last step calculates σ and ε as described in chapter 4.2.

Testing this program on theoretically calculated signals show that the program has difficulties on determining the correct ε and σ for some values. A test with Fourier-coefficients 1-10 is made and the 3rd and the 5th coefficients are found to give the most accurate result. However, the program still have difficulties identifying the correct values for some ε and σ. There are multiple reasons for this error. Firstly, the system of equations is badly conditioned for the outer regions of the $\sigma\varepsilon$-matrices. Secondly, the numerical accuracy from the FFT-analysis and the several interpolations made in the program, could be a source of error. It is discovered that the error is not random, i.e. a trend exists. Therefore a correction-matrix is calculated. This matrix is obtained by identifying signals with known ε and σ. The error from the correct values of ε and σ is then stored in a matrix, which is used for correction of the calculated values of ε and σ in the main program.

6 Test phase

The measurements are performed on a steel bar and a hand made model of a crack, see Figure 6.1. Since no rupture-testing machine is available, the steel bar is simply bent back and forth to introduce micro-cracks. As signal-source a shaker is used and as gauge an ICP pressure sensor and an accelerometer. The reason for choosing a piezoelectric pressure sensor is that they are characterised by their ability to measure extremely fast pressure fluctuations, and can accurately sense small dynamic pressure fluctuations.

To maximise the input amplitude it is desirable that the excited frequency is a resonant frequency of the test object. This fact forces us to use rather high frequencies when measuring on the steel bar, i.e. 40-50 kHz. Pressure sensors are generally linear over a wide dynamic range, this particular one 8.3-500 kHz, which satisfies our needs. A test on the steel bar is also made with two input frequencies, according to [12,13]. This test is made for empirical reasons only, i.e. to see if this method provides a more sensitive way of crack-detection. The investigation is limited to graphical interpretation of an FFT-analysis of the measured signal. For the measurements on the crack model, an accelerometer is used because of the much lower input frequencies. To make sure the test object is non-linear, a simple model of a crack is made, see Figure 6.1.

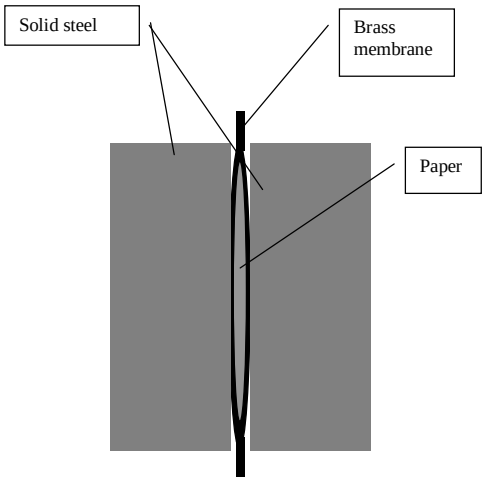

Figure 6.1. Handmade test object.

A brass membrane with paper in between and two weights build up this device. The device will vibrate as an excitation signal is applied and thereby change the contact surface area. This ensures us that the test object is indeed non-linear. The reason for putting paper inside the membrane is that we can avoid the harsh metal to metal contact and get a smoother transfer of the wave. Note that this does not remove the non-linear effect, it simply removes the most extreme wave amplitudes. This simple model of a crack enables the use of much lower excitation frequency. The required power from the signal source is obviously also lower than for a solid material with cracks.

6.1 Test Equipment

The equipment used for this experiment is shown in table 6.1.

Table 6.1. Test Equipment

Shakers	Ling Dynamic Systems, V201/3 and V406/8
ICP Pressure Sensor	Piezotronics, PCB 132A31
ICP-amplifier	Piezotronics, PCB 480C02
Digital Oscilloscope	Hitachi, VC6025A
Digital Measuring system	Hewlett Packard, 35650
Accelerometer	DYNATRAN, 3220A
Steel bar	5x5x400
Crack model	Brass plate and steel weight

The shaker's frequency response is from DC to 9 kHz. It is, however, capable of much higher frequencies (up to 50 kHz) but is no longer in its linear range. This is, however, not considered a problem since the linearity only concerns the amplitude, and not the wave shape.

The pressure sensor has a frequency range from 8.3 kHz to 500 kHz. This fact limits our selection of input excitation frequency to 8.3-50 kHz for the steel bar. The chosen excitation frequency, however, is a resonant frequency of the test system. The oscilloscope has capabilities of a sampling frequency up to 20 Msps. The digital output however, is limited

to a resolution of eight bits and 1000-4000 samples, depending on the number of active channels etc. The accelerometer has a linear response range from 50 to 3000 Hz.

6.2 Test Procedures

6.2.1 One Input Frequency

The measurements are conducted with a shaker as signal source and an ICP pressure sensor or an accelerometer as a gauge. The shaker is glued to the test object and the sensor is attached at the opposite end with wax.

A sinusoidal signal is then applied to the test object by the shaker and the propagated signal is measured with the sensor. The input frequency is chosen to one of the systems resonant frequencies. This is done in order to retrieve an output signal. If the input frequency is chosen differently, the wave amplitude is hardly measurable. This is due to the low output from the shaker at this frequency (40-50 kHz). Note that the input frequency is the resonant frequency for the system, and not for the steel bar alone. This is a disadvantage when trying to maximise the wave amplitude in the non-linear media (the steel bar). The data from the measurements are transferred from the digital oscilloscope to a PC.

6.2.2 Two Input Frequencies

When using two input frequencies, shakers are attached at both ends and the sensor is attached to the side of the test object.

Two sinusoidal signals are then applied to the test object by the shakers and the propagated signal is measured with the sensor. The high frequency input signal is chosen to one of the systems resonant frequencies. This is done in order to retrieve an output signal. If the input frequency is chosen differently, the wave amplitude is hardly measurable. This is due to the low output from the shaker at this frequency (40-50 kHz), which forces us to use the systems resonant frequency. Note that the input frequency is the resonant frequency for the system, and not for the steel bar alone. This is a disadvantage when trying to maximise the wave amplitude in the non-linear media (steel bar).

6.3 Test set-up

An overview of the equipment set-up is seen in Figure 6.2.

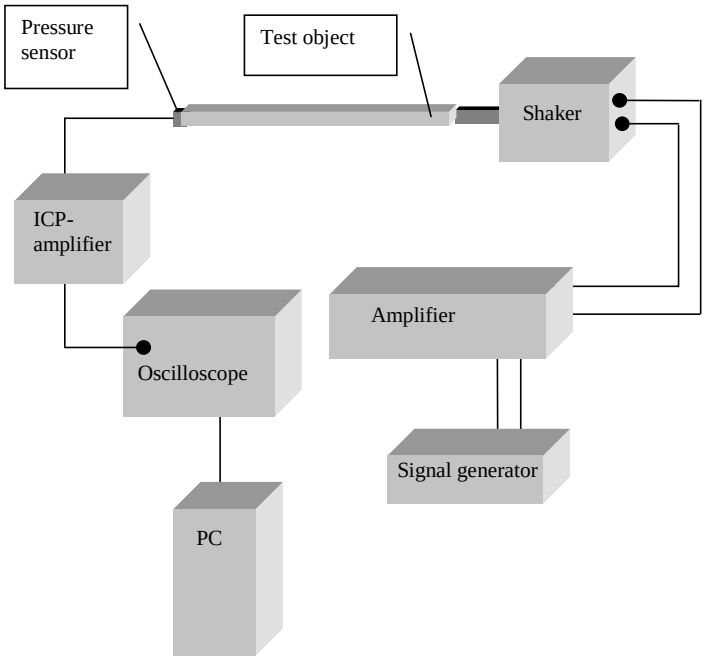

Figure 6.2. Test set-up overview.

The hand made crack model set-up is seen in Figure 6.3

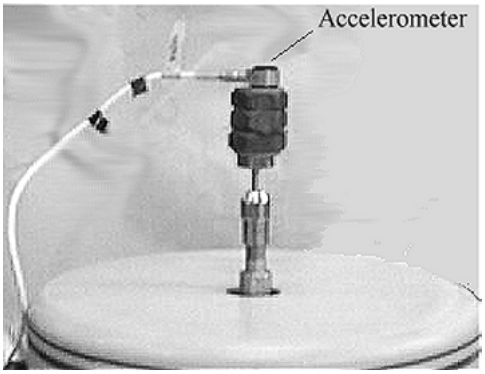

Figure 6.3. Test set-up for crack model.

The accelerometer is attached with wax on top of the hand made crack model and the shaker is glued to the opposite end.
The same set-up is used for the steel bar when using one excitation frequency.

When using Sutin's method with two input frequencies, two shakers are attached at opposite ends of the test object and the sensor is attached on the side of the object, see Figure 6.4.

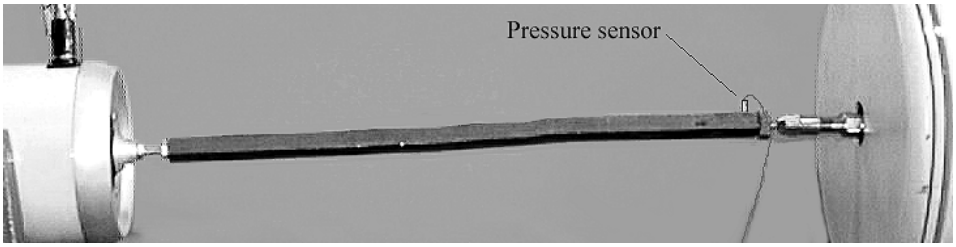

Figure 6.4. Test set-up. Two input frequencies.

6.4 Test results

Testing with steel bars shows no detectable quadratic non-linearity. The reason for this is probably the limited output power from the shaker. A more powerful piezo actuator would perhaps have been able to reveal the non-linearity, see [13]. However, a different effect is discovered. A quadratic non-linear effect would have shown itself as frequency components located around the high frequency with multiples of the low frequency, see Figure 6.5.

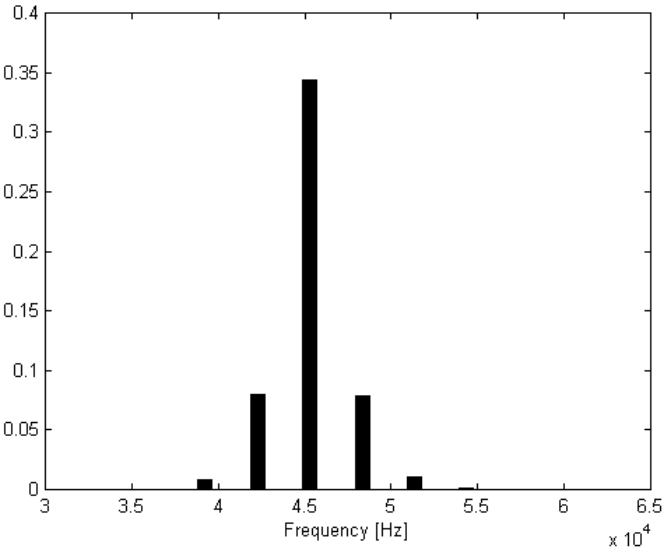

Figure 6.5. FFT of theoretical signal. Two input frequencies, 3 and 45 kHz.

The measured signal shows a broad continuous frequency spectrum with diminishing amplitudes around the high frequency, see Figure 6.6. Using one frequency shows a similar result.

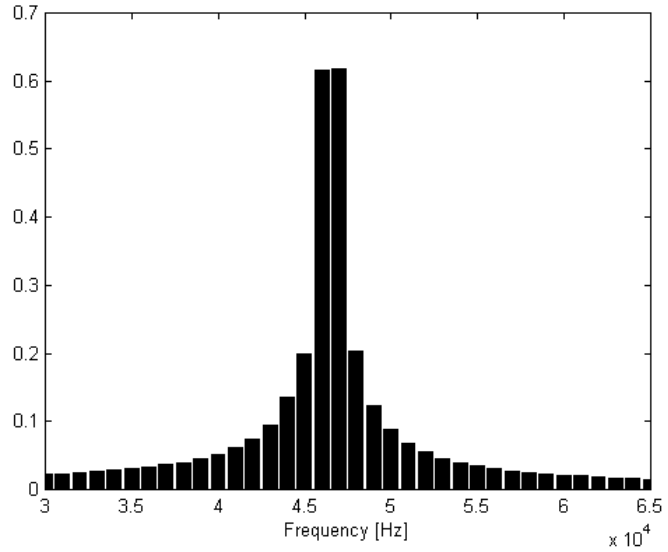

Figure 6.6. FFT-analysis for steel bar. Two input frequencies, 2 and 46 kHz. Steel bar submitted to high tension.

Figure 6.7 shows the corresponding measurement for a steel bar that has not been submitted to high tension. Note the lack of frequencies around the high frequency component.

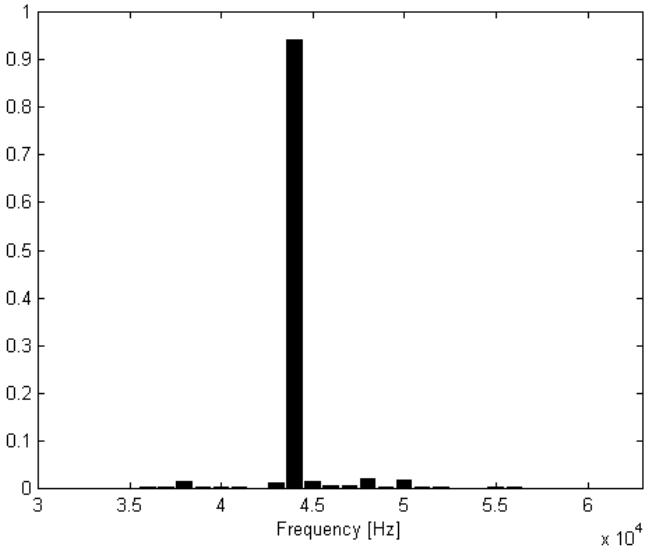

Figure 6.7. FFT-analysis for steel bar. Two input frequencies, 2 and 44 kHz. Steel bar not submitted to high tension.

Testing with the hand made crack model shows more expected results. As can be seen in Figure 6.8, the time response shows the more saw-tooth like shape that is characteristic for a quadratic non-linearity. The positive peaks have moved to the right and the negative to the left, i.e. positive amplitudes propagate faster than negative ones.

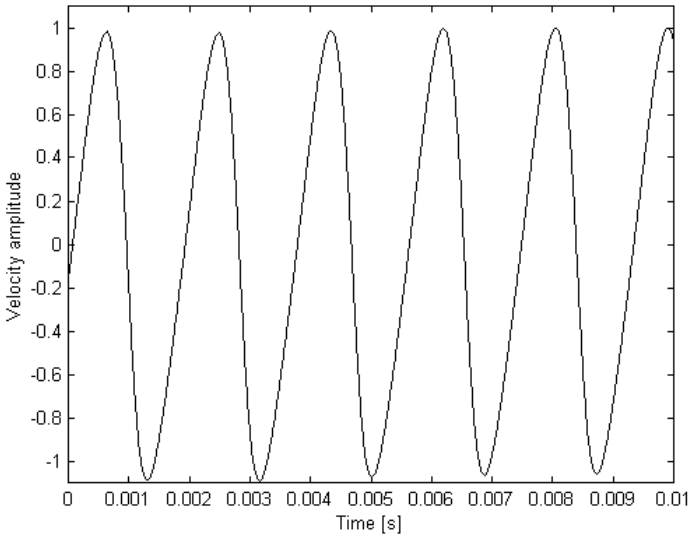

Figure 6.8. Time response signal for hand made crack model. Excitation frequency 540 Hz.

The frequency spectrum of the signal in Figure 6.9 also shows that higher harmonics with multiples of the input frequency have been created.

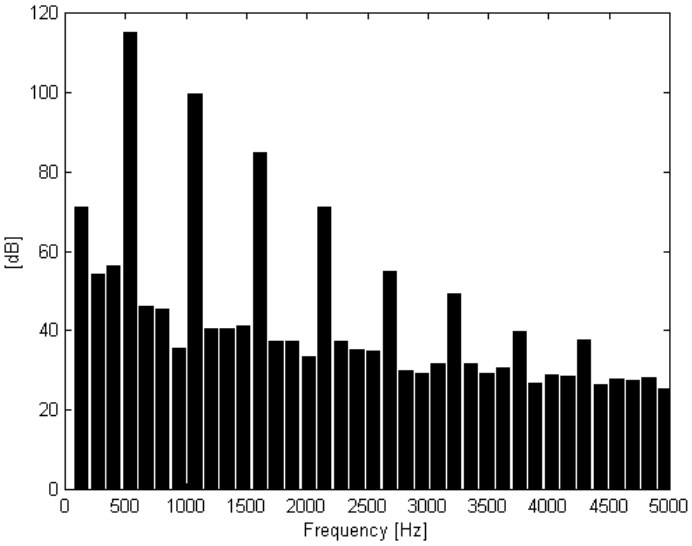

Figure 6.9. Frequency spectrum for hand made crack model. Excitation frequency 540 Hz.

Analysing this wave, using the identification program, gives ε =0.4 and σ =0.7. The real parameter values are easily determined with eq. 4.2-4.7. This is not done in this case since the real parameters have no useful physical meaning.

7 Discussion

The investigated method works well for the hand made crack. Propagating a sinusoidal wave through the “crack” clearly shows a non-linear response. Testing with a steel bar did not turn out quite that well. The shaker’s power output in the frequency range 40-50 kHz, used for the steel bar, is probably too low. A more powerful piezo actuator would probably have been able to vibrate the object to such an extent that the micro cracks would “open and close”. A piezo actuator has been used successfully in earlier experiments [12,13].

Despite this failure, a different phenomenon is discovered when testing with the steel bar: The measured signal shows a broad continuous frequency spectrum with diminishing amplitudes around the high frequency. According to A. Sutin, in a private communication: “The reason for this effect is not yet investigated. Other observations of this phenomenon is made, but without theoretical interpretation. A possible explanation is that high frequency signal simulates acoustical emission signals. These emission signals interact with the high frequency signal and give the modulation”. The investigation of this effect, however, is beyond the scope of this paper.

The method investigated can be used to detect the presence of a crack or cracks, but it cannot determine its position. This is often a high priority in non-destructive testing. Non-linear acoustic methods can be improved for this purpose. The simplest option is to use the standard echo ranging principle. Radiation and reception of the pulse sinusoidal signal is performed. However, as distinct from the standard echo ranging, the reflected signal is received at the frequency of the second harmonic of the radiated signal. In the case of scattering of an acoustic wave by the crack, the amplitude of the second harmonic may well be much greater than the level of the second harmonic generated in a homogeneous medium. It is precisely this fact that provides reliable separation of the useful signal against the interference background. The method presented helps to determine the location of the crack in the case of strong linear reflections of acoustic waves from other inhomogeneities, for example, the boundaries of the medium. Such a method has already been applied in the diagnostics of gas-bubbles in the sea.

Another scheme according to which the crack position is determined by non-linear methods is based on the modulation of a continuous signal by a more powerful pump pulse. The central idea of the method can be formulated as follows: a more powerful pump pulse passing through a crack changes its opening, and as a result of its non-linearity, changes the conditions of reflection and transmission for a continuous sounding wave. In this case, an additional reflection from the crack can occur, and the phase of the transmitted wave can change. Accordingly, possible patterns of non-linear tomography can be based on the registration of reflected or transmitted waves.

In the pattern based on the reception of a reflected wave, the radiation of the signal and pump waves occurs on one side of the object studied. When a pump pulse passes through a crack, the reflection factor for the signal changes, which brings about an additional scattered field. This field shows up only at the moment the pump pulse passes through the crack and can be determined even against the background of a strong stationary reverberation. The distance to the crack is determined by the time t_1 of the reflected signal's delay relative to the time of the pump pulse radiation and is equal to $2t_1c_0$, where c_0 is the velocity of acoustic waves in the object in question.

A second set-up is possible: the test harmonic is radiated on one side of the object, while radiation of the pump pulse and reception of the signal wave are performed on the other side. Upon reception, the phase modulation of the signal wave due to the modulation of the crack elasticity is separated. Here the distance is also determined by the time t_2 elapsed from radiation of the pump pulse to arrival of the phase-modulated signal wave and equals $2t_2c_0$.

8 Conclusions

In this work a theoretical model for identification of acoustical non-linearity using Burger's equation was implemented in a MATLAB program. The program identified both the non-linearity parameter and the distance from the signal source. Tests were performed in order to verify the theories.

The investigated method worked well for the hand made crack. Propagating a sinusoidal wave through the “crack” clearly showed a non-linear response. Testing with a steel bar did not turn out quite that well. The shaker’s power output in the frequency range 40-50 kHz, used for the steel bar, was probably too low. A more powerful piezo actuator would probably have been able to vibrate the test object to such an extent that the micro cracks would “open and close”. A piezo actuator has successfully been used in earlier experiments [12,13].

Despite this failure, a different phenomenon was discovered when testing with the steel bar: The measured signal showed a broad continuous frequency spectrum with diminishing amplitudes around the high frequency. According to A. Sutin, in a private communication: “the reason for this effect is not yet investigated. Other observations of this phenomenon is made, but without theoretical interpretation. A possible explanation is that high frequency signal simulates acoustical emission signals. These emission signals interact with the high frequency signal and give the modulation”. The investigation of this effect, however, is beyond the scope of this paper.

9 References

1. Blackstock David T., *Connection between the Fay and Fubini Solutions for Plane Sound Waves of Finite Amplitude*. The Journal of the Acoustical Society of America, 1966, vol. 39/6 p.1019-1026.
2. Blackstock David T., *Thermoviscous Attenuation of Plane, Periodic, Finite Amplitude Sound Waves*. The Journal of the Acoustical Society of America, 1964, vol. 36 p. 534-542.
3. Datta S.K., Achenbach J.D. and Rajapakse Y.S., *Elastic Waves and Ultrasonic Non-destructive Evaluation*. Elsevier Science Publishers B.V., 1990.
4. Fay R. D., *Plane Sound Waves of Finite Amplitude*. The Journal of the Acoustical Society of America, 1931, vol. 3, p.222-241.
5. Fubini-Ghiron E., *Anomalie nella propagazione di onde acustiche di grande ampiezza*. Alta Freq. 1935, 4, p. 530-581.
6. Hedberg Claes M., *Theoretical Studies of Non-linear Propagation of Modulated Harmonic Sound Waves*. Royal Institute of Technology Department of Mechanics, Doctoral Thesis 1994.
7. Hedberg Claes M., *Parameter Sensitivity in Non-linear and Dissipative Time-reversed Acoustics*. Proceedings of 16th ICA/135th ASA. Seattle 20-26th June 1998, p.543-544.
8. Korotkov A., Slavinsky M., Sutin A. M., *Non-linear Vibro-Acoustic Method for Diagnostics of Metal Strength Properties*. Advances in Nonlinear Acoustics. Ed. H.Hobæk. World Scientific. Singapore-New Jersey-London-Hong Kong. 1993, p. 370-375.
9. Mendousse J. S., *Non-linear Dissipative Distortion of Progressive Waves at Moderate Amplitudes*. The Journal of the Acoustical Society of America, 1953, vol. 25/1 p. 51-54.
10. Naugolnykh K., Ostrovsky L., Nonlinear *Wave Processes in Acoustics*. Cambridge University Press, 1998.
11. Rudenko O.V. and Soluyan S.I., *Theoretical Foundations of Nonlinear Acoustics*. Moscow State University, 1975.
12. Sutin A. M., *Nonlinear Acoustic Non-destructive Testing of Cracks*. Non-linear Acoustics in Perspective, 14th – intern. Symp. On Non-linear Acoustics. Ed. R.J. Wei Najing University Press, China, 1996, p. 328-333.

13. Sutin A. M. and Nazarov V. E., *Non-linear Acoustic Methods of Crack Diagnostics*. Radio Physics & Quantum Electronics, 1995, v.38, n.3/4, p. 109-120.

Department of Mechanical Engineering, Master's Degree Programme
University of Karlskrona/Ronneby, Campus Gräsvik
371 79 Karlskrona, SWEDEN

Telephone: +46 455-78016
Fax: +46 455-78027
E-mail: Goran.Broman@ima.hk-r.se